Journal of Theoretical Biology 527 (2021) 110814

Contents lists available at ScienceDirect

Journal of Theoretical Biology

journal homepage: www.elsevier.com/locate/yjtbi

Population dynamic regulators in an empirical predator-prey system

A. Frank [a], S. Subbey [b,c,*], M. Kobras [d], H. Gjøsæter [b]

[a] Computational Biology Unit, Dept. of Informatics, University of Bergen, PO Box 7803, 5020 Bergen, Norway
[b] Inst. of Marine Res, PO Box 1870, 5817 Bergen, Norway
[c] Western Norway University of Applied Sciences (HVL), PO Box 7030, 5020 Bergen, Norway
[d] Dept. of Mathematics and Statistics, University of Reading Whiteknights, PO Box 220, Reading RG6 6AX, UK

ARTICLE INFO

Article history:
Received 24 August 2020
Revised 13 May 2021
Accepted 13 June 2021
Available online 20 June 2021

Keywords:
Delay differential equations
Hopf bifurcation
Optimization
Match-Mismatch
Barents sea capelin

ABSTRACT

Capelin (Mallotus villosus) is a short-lived (1–4 years) fish species, that plays a crucial role by dominating the intermediate trophic level in the Barents Sea. Several episodes of extreme biomass decline (collapse) have been observed during the last three decades. We postulate that these collapses might be regulated by food availability (bottom-up effect) and/or by time discrepancy between capelin feeding and abundance of its prey (match-mismatch hypothesis). This paper investigates our postulate using a model consisting of a set of coupled differential equations to describe the predator-prey system, with a single delay term, τ, in description of the predator dynamics. We derive theoretical conditions on τ, as well as determine how changes in these conditions define different stability regimes of the system. Unconstrained optimization is used to calculate optimal model parameters by fitting the predator-prey model to empirical data. The optimization results are combined with those from the theoretical analysis, to make inference about the empirical system stability. Our results show that Hopf bifurcation occurs in the predatory-prey system when τ exceeds a theoretically derived value $\tau^* > 0$. This value represents the critical time for prey availability in advance of the optimal predator growth period.Set into an ecological context, our findings provide mathematical evidence for validity of the match-mismatch hypothesis and a bottom-up effect for capelin.

1. Introduction

Capelin (Mallotus villosus) is a short-lived (1–4 years) fish species with a northern circumpolar distribution (Carscadden and Vilhjálmsson, 2002) that spawn only once in their lifetime and then die (Gjøsæter et al., 2002b). The species is a forage fish (Buren et al., 2014) and play a crucial role by dominating the intermediate trophic level in their respective ecosystems. Such species are sometimes called "wasp-waist species" and are partly controlled by bottom-up, partly by top-down effects (Cury et al., 2000; Bakun, 2006; Hunt and McKinnell, 2006; Buren et al., 2014). The largest capelin stock belongs to the Barents Sea ecosystem (Gjøsæter Bogstad, 1998) and plays a crucial role there as the dominant feeder on zooplankton, which enters the Barents Sea via the Atlantic water influx (Ingvaldsen and Gjøsæter, 2013). Capelin is furthermore an important prey for larger fish, sea mammals and birds. Its selected prey size and type is age-dependent (Gjøsæter et al., 2002b). Capelin is preferred prey for the Northeast Arctic cod (Gjøsæter et al., 2009). Several episodes of extreme capelin biomass decline (collapse) have been observed in the Barents Sea during the last three decades. Large predation (top-down effect) from other species (during crucial capelin life stages) (Gjøsæter Bogstad, 1998; Hamre, 1991) has served as one explanation for these episodic events of collapse. Though the literature also reports that food availability (bottom-up effect) may be regulatory to the capelin population dynamics (see e.g., Gjøsæter et al., 2002b), this effect has been assumed to be of less significance, compared to the top-down effect. However, recent statistical analysis results (Solvang et al., 2017) have shown that there is a significantly strong link between the dynamic evolution of the biomass of capelin and that of its prey. The analysis did not extend to understanding the characteristics of this link and the existence of different regulatory conditions that may lead to different biomass states. Mathematically, such bottom-up effects can be modeled using predator-prey models (Ruan, 2009).

If $x \in \mathbb{R}_{\geqslant 0}$ and $y \in \mathbb{R}_{\geqslant 0}$ are state variables that represent population indices (e.g., abundance) respectively, of prey and predator, then the classical Lotka-Volterra Model (LVM) (Lotka, 1926; Volterra, 1926) description of the system, $V(\dot{x}, \dot{y})$, is defined by

* Corresponding author at: Inst. of Marine Res, PO Box 1870, 5817 Bergen, Norway.
E-mail addresses: Anna-Simone.Frank@uib.no (A. Frank), samuels@hi.no (S. Subbey), m.kobras@pgr.reading.ac.uk (M. Kobras), harald@hi.no (H. Gjøsæter).

https://doi.org/10.1016/j.jtbi.2021.110814
0022-5193/

$$V(\dot{x},\dot{y},\boldsymbol{\theta}_x,\boldsymbol{\theta}_y) \equiv \begin{cases} \dot{x} = F(x,y,\boldsymbol{\theta}_x), \\ \dot{y} = G(x,y,\boldsymbol{\theta}_y), \end{cases} \tag{1}$$

where $F : \mathbb{R}_+ \to \mathbb{R}_+$ and $G : \mathbb{R}_+ \to \mathbb{R}_+$ are continuous functions, and $\boldsymbol{\theta}_x \in \mathbb{R}^n$ and $\boldsymbol{\theta}_y \in \mathbb{R}^m$ are sets of parameters associated with x and y, respectively. Several theoretical analyses in the current literature (see e.g., Guan et al., 2018; Bakare et al., 2018; Freedman and Waltman, 1977) determine how $\boldsymbol{\theta}_x$ and $\boldsymbol{\theta}_y$ influence system dynamics.

Following e.g., Bazykin (1998), -we can define

$$\begin{cases} F(x,y,\boldsymbol{\theta}_x) = ax - bxy - ex^2, \\ G(x,y,\boldsymbol{\theta}_y) = -cy + dxy - hy^2, \end{cases} \tag{2}$$

then $\boldsymbol{\theta}_x \equiv \{a,b,e\}$, and $\boldsymbol{\theta}_y \equiv \{c,d,h\}$. In (2), the term $ax - ex^2$ defines a logistic growth with a limiting carrying capacity a/e (see e.g., Verhulst, 1838), and bxy is loss in prey biomass due to predation, also known as the functional response (Holling, 1959). The predator dynamics are determined by a natural death rate term cy, population decrease due to intraspecific competition hy^2, and dxy, which defines the biomass gain through predation.

Since the parameters in $\boldsymbol{\theta}_x$ and $\boldsymbol{\theta}_y$ determine the trajectory of the state parameters, their definition is reflective of the underlying ecological assumptions. Thus, one may constrain any $\theta \in \boldsymbol{\theta}_x$ (similarly for $\boldsymbol{\theta}_y$) to a scalar domain in $\mathbb{R}$ or to the domain of some continuous function in $\mathbb{R}$.

Seasonality is an important characteristic feature of e.g., boreal and arctic environments for population growth (Hanski et al., 1993; Hanski et al., 2001) and an obvious driver of the system (see e.g., Stickney, 1991). For example, the authors in Turchin and Hanski (1997) assumed that seasonality has continuous time effect by defining growth rates, both a and c, as smooth sine functions of time. However, incorporating such information in the population dynamics (of either predator and/or prey) may be generally, non-trivial, especially as different functional expressions of the seasonality may lead to different scenarios of the population trajectory (Rinaldi et al., 1993).

Another ecological consideration is the fact that a time delay exists between when prey is ingested, until it is converted to predator biomass. The simplest approach to addressing this consideration is to introduce a constant delay $\tau > 0$ in the predation term of the predator (Sarwardi et al., 2012), so that $G(x,y,\boldsymbol{\theta}_y)$ is redefined as

$$G(x,y,\boldsymbol{\theta}_y) = -cy + dx_\tau y - hy^2, \tag{3}$$

where in general, we use the notation $x_\tau \equiv x(t-\tau)$.

The model in (1) is a simplification of Sarawadi's model (Sarwardi et al., 2012) without a functional response, and y_τ in the equation for predator dynamics. We chose this simplification due to the assumption that changes in predator biomass take much longer time compared to the time it takes to digest prey. In this way, we assume that biomass for predator was "constant" at time $t-\tau$, when prey was consumed, and we could therefore neglect term y_τ in the predator change equation. This simplification, in essence, makes our model similar to the models by Beretta and Kuang (1996), which includes one time-lag for gestation in the predation term. The ecological significance of this time-window deals with the match-mismatch hypothesis (MMH) (Cushing, 1990), which asserts that dynamical variations in a population are driven by the relationship between its phenology (i.e., timing of population seasonal activities) and that of the immediate lower trophic level species. Normally, the MMH is limited to deal with mortality of fish larvae during their critical early life stages. However, the concept may be broadened to include other life history parameters than mortality, e.g. growth and maturation, and the original temporal aspects may be broadened to include also spatial aspects of match and mismatch, as exemplified above. In contrast to our formulation, other predator-prey model types include delays, for example, in the interaction term between prey and predator (see Sarwardi et al., 2012; Frank, 2017). Such models make the assumption that there was certain amount of prey and predator biomass, τ time-steps prior, and that also predator biomass influences prey consumption. Yet another predator-prey model type includes additional delays in, for instance, the maturation terms of the prey (Ruan, 2009). A more comprehensive review of different predator-prey models with discrete delays and their complex dynamics can be found in Ruan (2009). Although the inclusion of delay-terms in predator-prey models might be ecologically sound (Sarwardi et al., 2012), the literature shows that time-lags have a destabilizing effect on the system dynamics (see Freedman and Rao, 1983; Frank, 2017). For example, when τ crosses a critical threshold, Hopf bifurcation might occur (Faria, 2001; Sarwardi et al., 2012).

For an empirical population where the integrated system may form the basis for inference about the population dynamics, an accurate estimate of τ is therefore important. Deriving the value of τ from empirical observations is, however, non-trivial. Yet, literature exists that calculates a critical delay (Sarwardi et al., 2012) or conditions for occurrences of bifurcations analytically (Faria, 2001).

predator-prey systems do not act in isolation of their environment. Environmental factors (biotic and abiotic) may act on different, individual time-scale resolutions, and feedback loops (i.e., different delay terms) to dictate the population dynamics (see e.g., Kroeker et al., 2013). Hence the system of equations with constant delay τ may be an approximation of one with infinitely distributed delays.

When data on both predator and prey are available, the parameters associated with F and G in (1) may be determined (as for example, in Muehlbauer et al., 2020) by numerical optimization. If $(\hat{x}_i, \hat{y}_i), i = 1,\ldots,n$, represent a set of empirical observations over n discrete time steps, and $\hat{x}_i = \hat{x}(\hat{t}_i)$ (similarly for $\hat{y}$), one may define the initial conditions for a system by setting $x(0) = \hat{x}_1$, and $y(0) = y_1$. One challenge is that, for the DDE system, τ and x at $t \in [-\tau,\ 0)$ must be known. Deriving these values from empirical observations may be non-trivial. Given fixed observation time intervals ($\Delta = \hat{t}_2 - \hat{t}_1 = \ldots = \hat{t}_n - \hat{t}_{n-1}$), $[0\ \Delta)$ and $[\Delta\ \infty)$ are two feasible intervals for τ. If the problem is formulated (using e.g., a constrained optimization approach) to include the estimation of τ, the derived solution will depend on the chosen feasible interval. In practice, empirical data are however not always available to test validity of ecological assumptions. In absence of data however, it would be especially restrictive to constrain parameter domains of the model. Also with partially available empirical data (only for either predator or prey, but not both), the estimation problem in (1) is challenging. Then auxiliary information is needed to validate the derived trajectory of the missing component.

The goal of this paper is to investigate whether the capelin biomass dynamics may be reconstructed (including episodic events of extreme decline) by solely considering a bottom-up regulation process and a single delay term, τ, in description of the predator dynamics. This delay term may be interpreted as the time delay between the changes in prey biomass and the corresponding changes in the capelin growth rate, while considering as instantaneous, the effect of capelin predation on its prey. See a similar consideration and approach in e.g., Bush and Cool (1976).

The paper adopts the model definitions in (2) and (3), and uses unconstrained optimization to estimate the parameters of the system. We make inference about the system dynamics using the derived parameters. The manuscript is organized in the following

way. Section 2 gives a summary of the observation data on which the modeling is based. Section 3 revisits the mathematical models, and presents their theoretic dynamical system analyses. This section also presents a formal definition of the optimization problem, whose solution yields the system parameters. The theoretical results inform inference on the predator-prey behavior, on the basis of the derived parameters. Section 4 gives an overview of the numerical experiments, whose results are presented in Section 5, and discussed in Section 6. Our conclusions and discussion about possible limitations of the results are presented in Section 6.1.

2. Data sources

From annual scientific cruises in the BS during September, data on species abundance, spatial distribution and demography have been obtained, since 1972 (Gjøsæter, 1998). The species abundance indices (length, weight, age, numbers) are converted into age-specific biomass.

Fig. 1 shows the biomass of capelin from 1972 to 2013 (for the indicated ages), with notable stock collapses in 1985–1989, 1993–1997, and 2003–2006 (Gjøsæter et al., 2009). This paper uses time series data of the age-structures capelin biomass (Fig. 1) as predator data..

For parameter estimation and modeling of predator dynamics, we use a time-series of capelin biomass data from 1990–2018. The data for age-4 capelin is excluded from the modeling because the observations are highly uncertain, infrequent, and low. Capelin biomass data are not reliable before 1983 (Gjøsæter et al., 2002a), and capelin biomass was extremely low between 1986–1989. Hence our simulations (and parameter estimation) start in 1990, when the stock has recovered (Tjelmeland, 1992).

We have used the term *prey* to collectively describe all capelin prey, with a wide repertoire from Arctic copepod species to Atlantic krill (Dalpadado et al., 2014). This decision is influenced by the following considerations. Firstly, we have considered the prey data as unavailable partly because we are unable to pin down the exact prey type. Secondly, the intensive feeding season for capelin is July–October (Gjøsæter, 1998). However, the scientific survey that collects data on the abundance of main capelin preys occurs at the end of this season.

Zooplankton species are major prey for the Barents Sea capelin (Dalpadado et al., 2012). Though major zooplankton communities are associated with influx of different water masses (of Atlantic, and Arctic origins), over 50% of the zooplankton that is advected into the Barents Sea is found to be correlated with the volume flux of Atlantic water (AW) (Ingvaldsen and Gjøsæter, 2013), measured at the Fugløya-Bear Island (FB) transect (along the Barents Sea opening). We therefore use data on normalized volume of Atlantic water influx, AWI, as proxy for the validation of the normalized modeled prey trajectory $x(\Theta_X^*, t)$.

All data used in this manuscript have been obtained from the database of the ICES Working Group on the Integrated Assessments of the Barents Sea (WGIBAR, 2019).

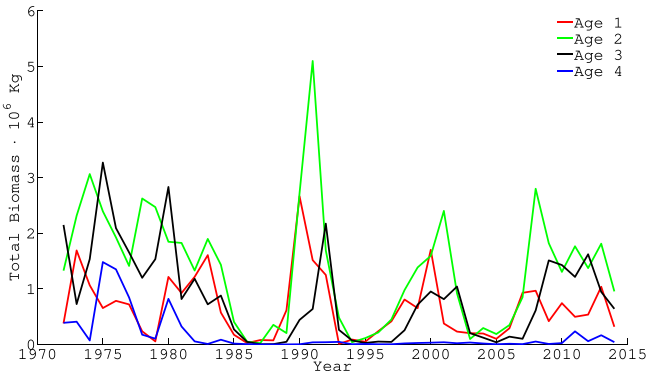

Fig. 1. The capelin biomass data.

3. Model and theoretical analyses

The main mathematical model description and theoretical analyses are presented in this section.

3.1. The general predator-prey model

We use the system in (1), where for $\tau \geqslant 0$, we define

$$\left.\begin{aligned} \dot{x} &= ax - bxy - ex^2, \\ \dot{y} &= -cy + dx_\tau y - hy^2, \end{aligned}\right\} \equiv V(\dot{x}, \dot{y}) \tag{4}$$

which are adaptations from Bazykin (1998) and Sarwardi et al. (2012).

3.2. Theoretical analyses of system dynamics

3.2.1. Coexistence and conditions

We use (4) to derive the non-trivial equilibrium point, $P_* \equiv (x_*, y_*)$, of the system $V(\dot{x}, \dot{y})$, which is given by

$$(x_*, y_*) \equiv \left(\frac{bc + ha}{bd + he}, \frac{ad - ce}{bd + he}\right), \tag{5}$$

where

- Condition 1 (**C1**): $ad > ce$

We linearize the system via

$$u(t) = x(t) - x_*, \; v(t) = y(t) - y_*,$$

to derive (6) from (4).

$$\left.\begin{aligned} \dot{u} &= -bx_* v - ex_* u \\ \dot{v} &= dy_* u_\tau - hy_* v \end{aligned}\right\} \equiv V(\dot{u}, \dot{v}) \tag{6}$$

Eq. (7) gives the characteristic equation for $V(\dot{u}, \dot{v})$,

$$\lambda^2 + p\lambda + q + re^{-\lambda\tau} = 0, \tag{7}$$

where $p = ex_* + hy_* \geqslant 0, q = hex_* y_* \geqslant 0$, and $r = bdx_* y_* \geqslant 0$. The equilibrium P_* is stable if all roots of (7) have negative real parts. For $\tau = 0$, we derive the characteristic Eq. (8), with discriminant $D = p^2 - 4(q + r)$.

$$\lambda^2 + p\lambda + q + r = 0. \tag{8}$$

Then the roots of (8) have (i) always negative real parts when $\{p > 0 \wedge D < 0\}$, (ii) always positive real parts when $\{p < 0 \wedge D < 0\}$, and (iii) at least one positive root for $\{p < 0 \wedge D \geqslant 0\}$. The constraining conditions are defined as

- Condition 2 (**C2**): $(ex_* + hy_*) > 0 \wedge (ex_* - hy_*)^2 < 4dbx_* y_*$, and
- Condition 3 (**C3**): $(ex_* + hy_*) < 0$.

3.2.2. Stability and bifurcation analysis

If we define $\lambda = iw$ as a root of (7), we derive (9)-(10)

$$-(w^2 - r\cos w\tau - q) + i(pw - r\sin w\tau) = 0, \tag{9}$$

$$w^4 + (p^2 - 2q)w^2 + q^2 - r^2 = 0, \tag{10}$$

which come from separating the real and imaginary parts. We introduce

$$z = w^2,\ \zeta = p^2 - 2q,\ \eta = q^2 - r^2$$

into (10), to arrive at (11)

$$z^2 + \zeta z + \eta = 0. \tag{11}$$

Note that $\zeta = p^2 - 2q > 0$ since $(p^2 - 4q) = (ex_* - hy_*)^2 \geqslant 0$, and the discriminant of (11), $D > \zeta^2$, for $q < r$. Hence, when $q < r$, (11) has a positive root, z_0, for $z \in (0,\ \infty)$, and no positive root when $r \leqslant q$. The positive root of (10), w_0 is then given by $\sqrt{z_0}$, i.e.,

$$w_0 = \sqrt{\frac{(p^2 - 2q)}{2}\left(-1 \pm \sqrt{\left[1 - \frac{4(q^2 - r^2)}{(p^2 - 2q)^2}\right]}\right)}. \tag{12}$$

Using the real part of (9), we define for $\kappa = 0, 1, 2, \ldots$

$$\tau_\kappa = \frac{1}{w_0}\left[\arccos\left(\frac{w_0^2 - q}{r}\right) + 2\pi\kappa\right], \tag{13}$$

and note that (7) with $\tau = \tau_\kappa$ has a pair of purely imaginary roots, $\pm i w_0$ for every τ_κ.

We investigate the transversality condition, expressed as Lemma 1.

Lemma 1. *Let $\lambda(\tau) = \alpha(\tau) \pm i w(\tau)$ be the root of (7) near $\tau = \tau_\kappa$, such that $\alpha(\tau_\kappa) = 0$, and $w(\tau_\kappa) = w_0$ for $\kappa = 0, 1, 2, \ldots$. Then if $q < r$,*

$$\left.\frac{d\mathrm{Re}\{\lambda(\tau)\}}{d\tau}\right|_{\tau=\tau_\kappa} > 0,\ \kappa = 0, 1, 2, \ldots \tag{14}$$

Proof. Rewrite (7) with explicit dependence of λ on τ, i.e., $\lambda \equiv \lambda(\tau)$, as

$$\lambda^2 + p\lambda + q + re^{-\lambda\tau} = 0. \tag{15}$$

Then

$$\frac{d\lambda}{d\tau} = \frac{r\lambda e^{-\lambda\tau}}{2\lambda + p - r\tau e^{-\lambda\tau}} = \left(\frac{(2\lambda + p)e^{\lambda\tau}}{r\lambda} - \frac{\tau}{\lambda}\right)^{-1} \tag{16}$$

However,

$$\begin{aligned} &\mathrm{Re}\left[\tfrac{\tau}{\lambda}\right]\Big|_{\lambda=\pm i w_0} = 0 \ \textit{and} \\ &\mathrm{Re}\left[\tfrac{(2\lambda+p)e^{\lambda\tau}}{r\lambda}\right]\Big|_{\lambda=\pm i w_0} = \tfrac{(p^2-2q)}{r^2} + \tfrac{2w_0^2}{r^2} \end{aligned} \tag{17}$$

since from (9),

$$\sin w_0 t = \frac{p w_0}{r},\ \cos w_0 t = \frac{(q - w_0^2)}{r}. \tag{18}$$

Finally, substituting for w_0 from (12), we deduce

$$\mathrm{Re}\left[\frac{(2\lambda + p)e^{\lambda\tau}}{r\lambda}\right]\Big|_{\lambda=\pm i w_0} = \underbrace{\frac{\sqrt{p^2(p^2 - 4q) + 4r^2}}{r^2}}_{>0}, \tag{19}$$

which completes the proof.

Theorem 1. *Let* **C1** *and* **C2** *prevail. Then all the roots (7) have negative real parts for $\tau \in [0,\ \tau^*)$, and P_* is asymptotically stable for $\tau \in [0,\ \tau^*)$. The system defined by (2) undergoes Hopf bifurcation at P_* when $\tau^* = \tau_\kappa,\ \kappa = 0, 1, 2, \ldots$*

Theorem 2. *Let* **C1** *and* **C3** *prevail. Then (7) has at least a root with positive real part for $\tau \in [0,\ \tau^*)$, and P_* is unstable for $\tau \in [0,\ \tau^*)$. The system defined by (2) undergoes Hopf bifurcation at P_* when $\tau^* = \tau_\kappa,\ \kappa = 0, 1, 2, \ldots$*

3.3. The optimization problem

The assumption that discrete empirical observations exist only for the predator, and not the prey, defines the optimization problem. Our goal is to determine the system parameter sets that minimize the discrepancy between modeled predator biomass and empirical data.

Define $\{i, n\} \in \mathbb{Z}_+$ such that $i = 1, \ldots, n$, and let $\hat{y}_i = \hat{y}(\hat{t}_i)$ represent empirical observations of y over n discrete time steps $\hat{t}_i$. Note that y and x are coupled (through the predation term). Furthermore, since we assume no data exists on $\hat{x}$, the initial condition $x(0)$ and delay term τ must be estimated as part of the optimization procedure. The trajectory of y will also depend on $x(0)$ and τ. Hence we write $y(\theta_x, \theta_y, x(0), \tau, t)$, and define Problem 1 as the general optimization problem.

Problem 1 (*The optimization problem*).

Determine $\boldsymbol{\theta} \equiv \{\theta_x, \theta_y, x(0), \tau\}$:

$$\underset{\boldsymbol{\theta}\in\mathbb{R}_{\geqslant 0}, t\in[0\ T]}{argmin} \|\hat{y}(t) - y(\boldsymbol{\theta}, t)\|, \tag{20}$$

where $\hat{y}(t)$ is known at $t = \hat{t}_1, \hat{t}_2, \ldots, \hat{t}_n \leqslant T$.

4. Description of numerical simulations

Determining the trajectories of the predator-prey system combines the problem of integrating the system of coupled DDEs, and deriving the solution, $\boldsymbol{\theta}^*$, of the optimization Problem 1. We use a numerical approach for integrating the DDE system, as for most of such coupled systems, finding closed form solutions is non-trivial (Bedziuk and Yablonski, 2010).

For the coupled DDE system, we use the Matlab dde23 algorithm, which is based on the ode23-solver, using the RKBS(2,3) method. Theoretical and computational details about dde23 can be found in Shampine and Thompson (2001). We set $y(-\tau) = y(0) = \hat{y}_1$, and $x(-\tau) = x(0) = x_0$. Since τ and x_0 are unknown, they are included in the parameter set $\boldsymbol{\theta}$ (see Problem 1).

We used the fminsearch algorithm in Matlab to derive the unconstrained model parameters. The fminsearch algorithm uses the Nelder-Mead algorithm (Nelder and Mead, 1965) to compute the unconstrained minimum of a given objective function. For a predefined tolerance ϵ, we consider the algorithm to have converged after J iterations when the change in the objective function $\Delta f(\boldsymbol{\theta}_j) < \epsilon$, for $j \leqslant J$. For each candidate solution, $\boldsymbol{\theta}_j$ $(j = 1, \ldots, J)$, spline-interpolated values of $y(\boldsymbol{\theta}_j, t)$ at n discrete (observation) points $\{\hat{t}_1, \hat{t}_2, \ldots, \hat{t}_n\}$ are obtained.

The objective function is then simply defined by (21).

$$f_j = \sum_{i=1}^{n} y(\boldsymbol{\theta}_j, \hat{t}_i) - \hat{y}(\hat{t}_i), \tag{21}$$

where, $f_j = f(\boldsymbol{\theta}_j)$. Based on the analysis presented in Section 3, we obtain system dynamics by analyzing the set of optimized parameters.

Finally, we validate the dynamics of the modeled prey trajectory, $x(\boldsymbol{\theta}_x^*, t)$, by comparing it to data on the normalized AWI.

5. Results

This section presents results from our numerical simulations for the DDE model. We adopt the following notations, some of which has been used in Section 3, but are repeated here for the sake of completeness and to ease readability:

x_0 represents the initial condition for prey, $\boldsymbol{v} = (a, b, c, d, e, h, \tau)$ is the parameter vector and the optimized parameter set is indicated with $\boldsymbol{v}^o$. τ^o is the optimized delay from the model fit to the data, τ^* is the critical delay, i.e., $\tau^* = \tau_k, k \geqslant 0$. Dependent on the optimized model parameters, we have the situation that either (i) $\tau^o < \tau^*$ (Theorem 2) or (ii) $\tau^o > \tau^*$ (Theorem 3) holds. For each of these cases we can illustrate dynamics for $\tau = \tau^o$ and $\tau = \tau^*$. However to show what happens with the dynamics when either $\tau > \tau^*$ (i) or $\tau < \tau^*$ (ii) we had to choose τ arbitrarily, and this is $\tau^\dagger$. For plotting the dynamics, the value of $\tau^\dagger$ was therefore chosen to be either above τ^* (i) or below τ^* (ii).

Table 1 shows results for our numerical simulations when $\tau > 0$. We used the optimized estimate of τ and results in Theorem 1 to calculate τ^*. Observe that results from the optimization show that it is Theorem 1 (and not Theorem 2) that applies to our empirical setting. Although we are able to calculate τ_κ, $\kappa \geqslant 0$, only τ_0 presents a biological realistic scenario, since capelin has a life-span of three years. The results presented in this section are therefore limited to the model dynamics for varying τ-values around $\tau^* \equiv \tau_0$. Fig. 2a.–b. shows the simulated prey and predatory biomass dynamics, as well as comparison between modeled and empirical predator biomass data. The DDE system is capable of replicating the empirical observations.

Fig. 2c. shows a consistent, temporal synchrony between the modeled and normalized prey biomass of age-3 capelin and the normalized AWI though large deviations (in absolute terms) exist between the two. Coherence between normalized modeled prey dynamics and AWI is less pronounced for ages 1 and 2 capelin, compared to the results for age-3 (see Figure A.1 in the appendix). However, the peaks in AWI overlap with peak-trends in biomass growth in the two younger age-groups, indicating also here a correlation between simulated prey and AWI.

Table 1
Parameter estimation results using data from 1990–2018 (age-1 and 3), and 1989–2018 (age-2). The optimization algorithm failed to converge for age-2 when data from 1989 was excluded – see discussion under Section 6

Age	$\boldsymbol{v}^o = (a, b, c, d, e, h, \tau^o)$	x_0	τ^*	$\tau^\dagger$
1	(1.1747, 2.0315, 0.750, 0.300, 0.0380, 0.3747, 0.1268)	16.2625	0.3204	0.5251
2	(0.4893, 0.3974, 0.9874, 0.2649, 0.0070, 0.1488, 0.0556)	13.1306	0.3860	0.7163
3	(0.5398, 0.8562, 1.0310, 0.2325, 0.0095, 0.0594, 0.1070)	8.9218	0.1473	0.1876

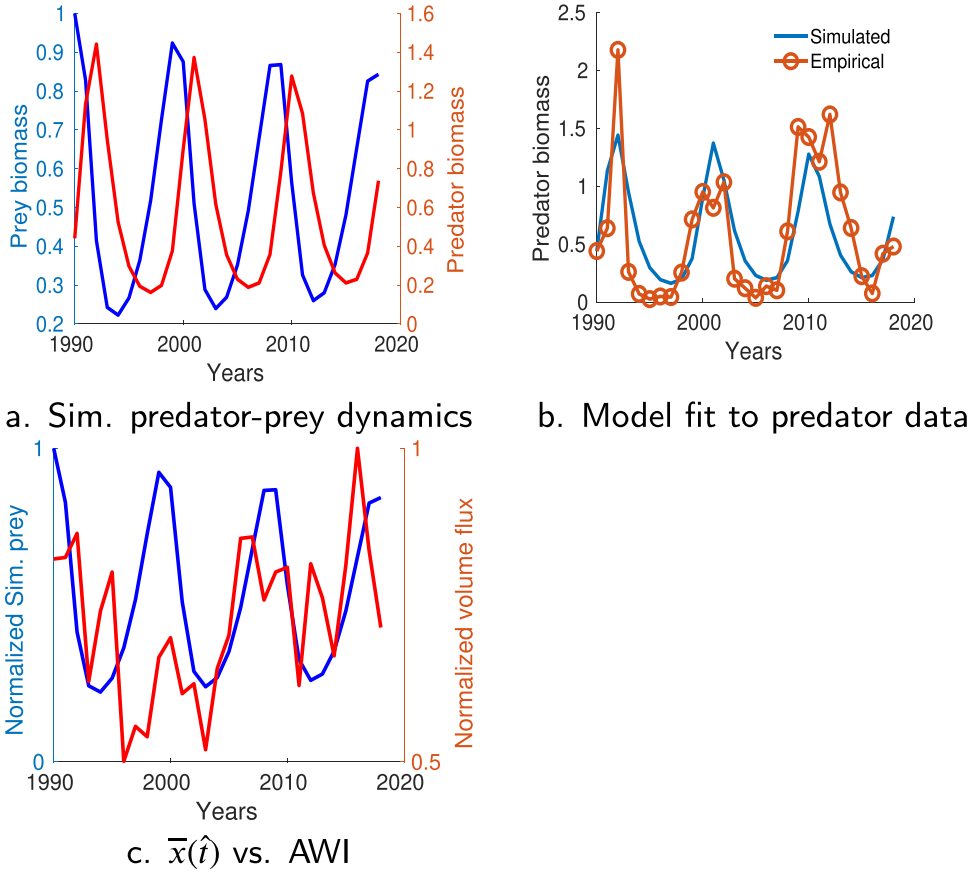

Fig. 2. DDE optimization results – Simulated predator-prey dynamics (a.), Model fit of predator dynamics to empirical data for age-3 capelin (b.), Scaled total biomass of prey, $\bar{x}(\hat{t})$, and normalized Atlantic water influx (AWI) (c.), in the period 1990–2018.

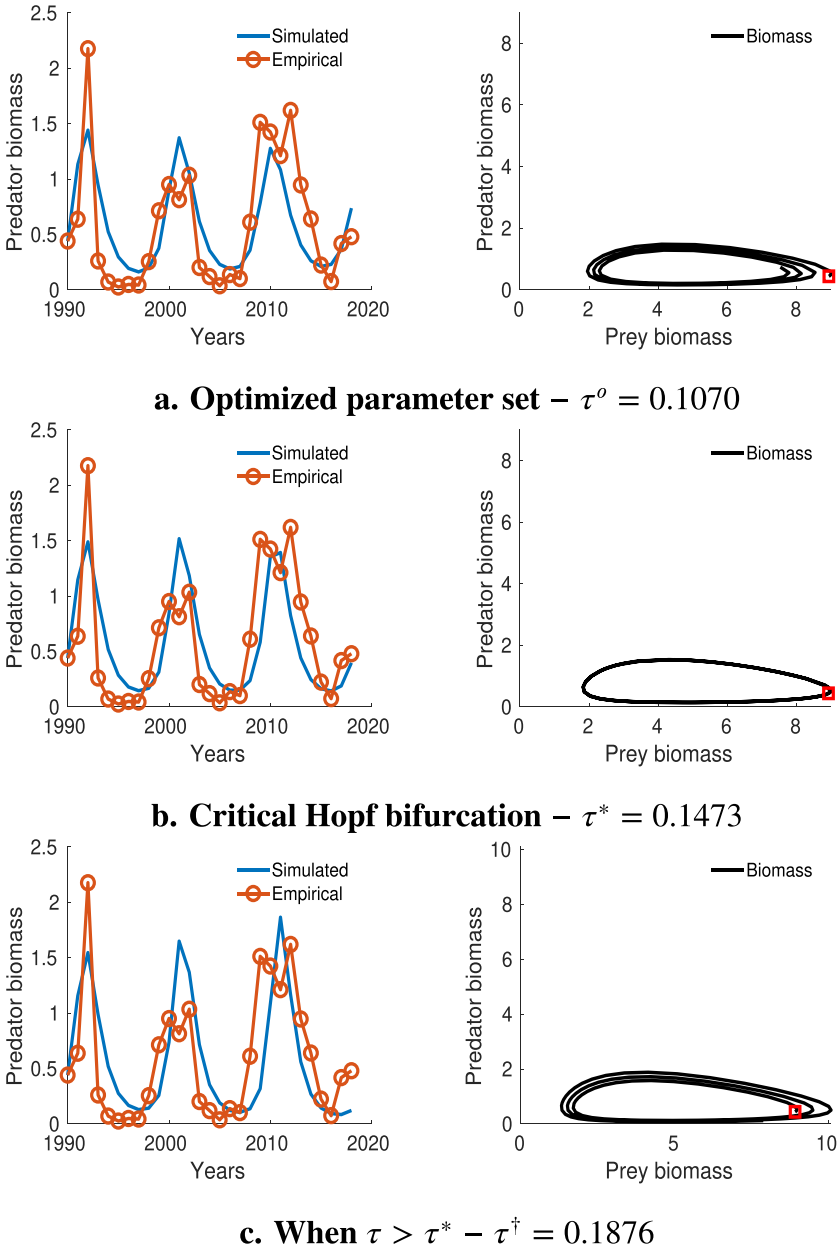

Fig. 3. τ-bifurcation analysis – **Left column:** Model fit to data (a.), Model simulations (b.)-(c.). **Right column:** Phase-plane plot of the predator-prey dynamics. Observe the phase-plane dynamic transitions from (a.) Asymptotic stable (τ^o) to (b.) A limit cycle (τ^*) to (c.) Asymptotic unstable ($\tau^\dagger$). The red square in the phase-plane plot is the origin of the time-series.

The first column in Fig. 3 shows fit of the DDE model to the data with the indicated τ values. The second column shows the corresponding phase-plane diagrams.

6. Discussion

This paper analyzed the dynamics of an empirical marine predator-prey system, both theoretically and numerically, based on Lokta-Volterra model formulations, where data on the prey is absent. We have used auxiliary information about the AWI to validate the modeled prey biomass dynamics. Although, full simulation results exist also for age-1 and age-2 capelin (Table 1), graphical results and discussions were focused on age-3 capelin. This has been done, partially for the sake of brevity. But most significantly, because the results for age-3 capelin are coherent and easier to interpret.

The modeled age-1 and age-2 prey dynamics could also be validated, albeit to a less degree of agreement, with data on AWI. The results might indicate that the younger age-groups may be regulated by bottom-up process to a lesser degree than age-3 capelin. This assumption, however, warrants further investigation that is beyond the scope of this manuscript.

In addition, for younger age-groups, more stochastic (e.g., defined by stochastic differential equations) prey model(s) may be required. Consequently, our modeled prey dynamics may represent a single realization of several stochastic dynamic prey trajectories.

In general however, we see good model fit to empirical data, for stable and unstable system equilibria (see Fig. 3).

Since **C1** and **C2** apply, Theorem 1 defines the condition for stability of the predator-prey system. This is confirmed by the results in Table 1 and Fig. 3, where for $\tau \in [0,\ \tau^*]$, the system dynamics is stable, but becomes unstable when $\tau = \tau^\dagger > \tau^*$.

Table 1 shows that the optimized delays (τ^o) and critical values (τ^*), are age-class dependent. Put together, these delay values define a time-window, $\Delta\tau \equiv [\tau^o,\ \tau^*]$, for stability of the predator-prey system. From (2), we note that for $\{c, d, h\} \geqslant 0$, the growth rate $G(x, y, \theta_y)$ at any time t satisfies (22),

$$G(x, y, \theta_y) \leqslant dy \cdot \max_{[t-\tau,\ t]}[x_\tau]. \tag{22}$$

Hence, predator growth is optimized when x_τ is maximum in $[t - \tau,\ t]$, for $\tau \in \Delta\tau$, and that this time-window is age-dependent. For the optimized time-delay window (in weeks), we observe that $\Delta_1\tau \equiv [8,\ 16], \Delta_2\tau \equiv [3,\ 16], \Delta_3\tau \equiv [4,\ 8]$, where Δ_j is the time-window for predator of age j.

Combining (22) and the results in this manuscript translate, in ecological terms, to mean that the growth rate (and stability) of the predator at any time t is determined by the size of prey biomass within $t - \Delta_j$ (for $j = 1, 2, 3$), weeks in advance. These differences in $\Delta\tau$ are reflective of the age- or length-specific feeding needs and prey types for capelin (see discussion in Gjøsæter et al., 2002b). An example of age-specific feeding needs of capelin is that age-1 capelin feeds on smaller zooplankton, while age-3 capelin prefers larger zooplankton species (Gjøsæter et al., 2002b; Dalpadado et al., 2014). The difference in food supply might explain the variations in the τ-window for the three age groups.

We extend interpretation of our results in an ecological context by firstly noting that feeding among fish is a dynamic process. A newly hatched capelin larva would, for instance, depend on availability of food objects of a narrow size spectrum. If such food (for instance eggs and young stages of crustacean plankton) is not available soon after the capelin larvae are hatched, they will have minimal chance to survive. In theory, similar mechanisms may exist also for older fish, but since they can choose among a wide range of food objects, they are much less prone to lack of suitable food. Adult fish are also extremely flexible as to when food is available; they may survive for long periods without eating anything, thanks to their low resting metabolism.

Our results show that the dynamic optimal growth rate (not necessarily the maximum) at any time t is determined by the size of prey abundance in the time-window $t - \Delta_j$ in advance. Note that what constitutes maximum predator growth rate is not only dependent on the prey abundance *per se, as growth rates may be dictated by other factors, e.g., ratio of prey to predator biomass, handling time, and optimal spatial overlap between predator and prey.*

Hence, optimal growth conditions might be a consequence of spatio-temporal overlap between prey and predator.

Though the MMH has gained acceptance, the literature lacks empirical evidence for its validity (see discussion in Durant et al., 2007). Our derived time windows, Δ_j, provide a possible link between capelin phenological growth and that of its prey. To the authors' knowledge, this is the first time such evidence of the MMH has been provided.

Although our results show that the observed cyclic variation in biomass of age-1 and older capelin is consistent with the hypothesized bottom-up regulation, this does not preclude the existence of top-down regulation both on early life stages (reviewed by Gjøsæter et al., 2016, and not dealt with in our modeling) or among adult capelin. The importance of bottom-up and top-down regulation might shift among various life history stages of capelin.

6.1. Conclusions

Our modeling results shed light onto the regulatory effect of prey on BS capelin biomass dynamics. Results from theoretical analyses and numerical simulations were consistent. We could also show that the simulated prey dynamics are synchronous with AWI, and have thus validated our model formulation of the prey.

Three key ecological highlights result from our analyses.

Firstly, we have presented results in support of a bottom-up regulation for the biomass dynamics of capelin age-1 and older. Secondly, based on combination of theory and simulations, we have identified time-frames for predator-prey overlap, which lead to optimal predator growth and stability of the predator-prey system. The identified time-frames differ for different age groups, and probably reflect age-specific feeding habits of the predator.

Thirdly, we have provided evidence, perhaps for the first time, of MMH applicability to capelin and its prey.

Our results present evidence that prey have strong regulatory effect on the biomass dynamics of predators of age-1 and older. However, we cannot infer from our results whether this can also partly explain the episodic collapses seen in the capelin biomass dynamics. In our opinion, such inference should be based on findings from this paper, combined with analyses of other biophysical information in space and time. However, this undertaking is beyond the scope of this paper and will therefore be investigated in a sequel paper.

CRediT authorship contribution statement

A. Frank: Conceptualization, Methodology, Software, Validation, Formal analysis, Investigation, Writing - original draft, Writing - review & editing, Visualization. **S. Subbey:** Conceptualization, Methodology, Software, Validation, Formal analysis, Investigation, Writing - original draft, Writing - review & editing, Supervision, Visualization. **M. Kobras:** Writing - review & editing, Visualization. **H. Gjøsæter:** Writing - review & editing.

Declaration of Competing Interest

The authors declare that they have no known competing financial interests or personal relationships that could have appeared to influence the work reported in this paper.

Acknowledgements

SS is grateful to the Fulbright Foundation (Norway) for funding his research at Cornell University, where work on this manuscript was initiated. Declaration of interest The authors declare that they have no conflicts of interest. Funding Sources This research did not receive any specific grant from funding agencies in the public, commercial, or not-for-profit sectors. Data statement All data used in this manuscript have been obtained from the database of the ICES Working Group on the Integrated Assessments of the Barents Sea (WGIBAR, 2019).

Appendix A

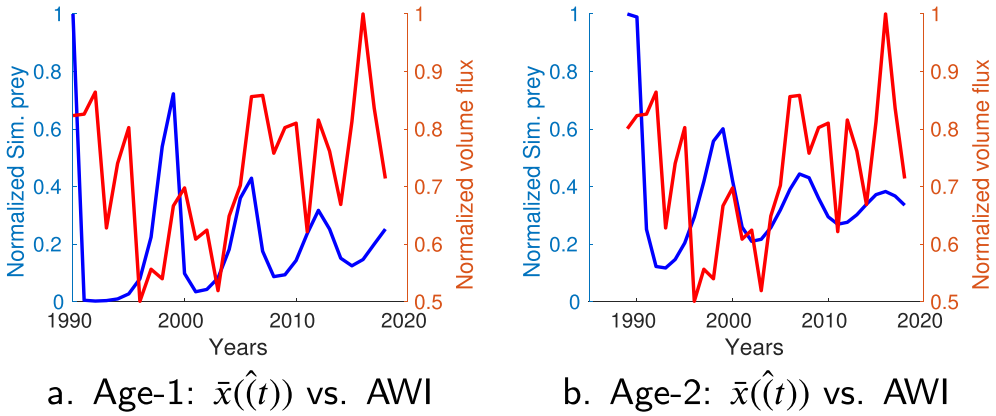

Fig. A.1. Scaled total biomass prey, $\bar{x}\left(\hat{(t)}\right)$ and normalized Atlantic water influx (AWI), for predator of age-1 (1990–2018) (a.), and age-2 (1989–2018) (b.).

References

Bakare, E., Chakraverty, S., Abolarin, O., 2018. Qualitative analysis and homotopy based solution of two species Lotka-Volterra model. Int. J. Pure Appl. Math. 119, 261–280. https://doi.org/10.12732/ijpam.v119i2.1.

Bakun, A., 2006. Wasp-waist populations and marine ecosystem dynamics: navigating the predator pit topographies. Prog. Oceanogr. 68, 271–288. https://doi.org/10.1016/j.pocean.2006.02.004.

Bazykin, A.D., 1998. Nonlinear dynamics of interacting populations volume 11.

Bedziuk, N., Yablonski, A., 2010. Solutions of nonlinear differential equations. Nonlinear Diff. Eq. Appl. 17, 249–270. https://doi.org/10.1007/s00030-009-0052-7.

Beretta, E., Kuang, Y., 1996. Convergence results in a well-known delayed predator-prey system. J. Math. Anal. Appl. 204, 840–853.

Buren, A.D., Koen-Alonso, M., Pepin, P., Mowbray, F., Nakashima, B., Stenson, G., Ollerhead, N., Montevecchi, W.A., 2014. Bottom-up regulation of capelin, a keystone forage species. PLoS One 9,. https://doi.org/10.1371/journal.pone.0087589 e87589.

Bush, A., Cool, A., 1976. The effect of time delay and growth rate inhibition in the bacterial treatment of wastewater. J. Theor. Biol. 63, 385–395. https://doi.org/10.1016/0022-5193(76)90041-2.

Carscadden, J., Vilhjálmsson, H., 2002. Capelin-what are they good for? introduction. ICES J. Mar. Sci. 5, 863–869. https://doi.org/10.1006/jmsc.2002.1283.

Cury, P., Bakun, A., Crawford, R.J., Jarre, A., Quinones, R.A., Shannon, L.J., Verheye, H. M., 2000. Small pelagics in upwelling systems: patterns of interaction and structural changes in wasp-waist ecosystems. ICES J. Mar. Sci. 57, 603–618. https://doi.org/10.1006/jmsc.2000.0712.

Cushing, D., 1990. Plankton production and year-class strength in fish populations: an update of the match/mismatch hypothesis, in: Advances in marine biology. Elsevier. volume 26, pp. 249–293. DOI: 10.1016/S0065-2881(08)60202-3..

Dalpadado, P., Arrigo, K.R., Hjøllo, S.S., Rey, F., Ingvaldsen, R.B., Sperfeld, E., Van Dijken, G.L., Stige, L.C., Olsen, A., Ottersen, G., 2014. Productivity in the barents sea-response to recent climate variability. PloS One 9,. https://doi.org/10.1371/journal.pone.0095273 e95273.

Dalpadado, P., Ingvaldsen, R.B., Stige, L.C., Bogstad, B., Knutsen, T., Ottersen, G., Ellertsen, B., 2012. Climate effects on barents sea ecosystem dynamics. ICES J. Mar. Sci. 69, 1303–1316. https://doi.org/10.1093/icesjms/fss063.

Durant, J.M., Hjermann, D.Ø., Ottersen, G., Stenseth, N.C., 2007. Climate and the match or mismatch between predator requirements and resource availability. Clim. Res. 33, 271–283. https://doi.org/10.3354/cr033271.

Faria, T., 2001. Stability and bifurcation for a delayed predator-prey model and the effect of diffusion. J. Math. Anal. Appl. 254, 433–463. https://doi.org/10.1006/jmaa.2000.7182.

Frank, A.S., 2017. Predictability of marine population trajectories–the effect of delays and resource availability. ESAIM: Proc. Surveys 57, 23–36. https://doi.org/10.1051/proc/201657023.

Freedman, H., Rao, V., 1983. The trade-off between mutual interference and time lags in predator-prey systems. Bltn Mathcal Biol. 45, 991–1004. https://doi.org/10.1007/BF02458826.

Freedman, H., Waltman, P., 1977. Mathematical analysis of some three-species food-chain models. Math. Biosci. 33, 257–276. https://doi.org/10.1016/0025-5564(77)90142-0.

Gjøsæter, H., 1998. The population biology and exploitation of capelin (Mallotus villosus) in the Barents Sea. Sarsia 83, 453–496. https://doi.org/10.1080/00364827.1998.10420445.

Gjøsæter, H., Bogstad, B., 1998. Effects of the presence of herring (clupea harengus) on the stock-recruitment relationship of barents sea capelin (mallotus villosus). Fish Res. 38, 57–71. https://doi.org/10.1016/S0165-7836(98)00114-3.

Gjøsæter, H., Bogstad, B., Tjelmeland, S., 2002a. Assessment methodology for Barents Sea capelin, Mallotus villosus (Müller). ICES J. Mar. Sci. 59, 1086–1095. https://doi.org/10.1006/jmsc.2002.1238.

Gjøsæter, H., Bogstad, B., Tjelmeland, S., 2009. Ecosystem effects of the three capelin stock collapses in the Barents Sea. Mar. Biol. Res. 5, 40–53. https://doi.org/10.1080/17451000802454866.

Gjøsæter, H., Dalpadado, P., Hassel, A., 2002b. Growth of Barents Sea capelin (Mallotus villosus) in relation to zooplankton abundance. ICES J. Mar. Sci. 59, 959–967. https://doi.org/10.1006/jmsc.2002.1240.

Gjøsæter, H., Hallfredsson, E.H., Mikkelsen, N., Bogstad, B., Pedersen, T., 2016. Predation on early life stages is decisive for year-class strength in the barents sea capelin (mallotus villosus) stock. ICES J. Mar. Sci. 73, 182–195. https://doi.org/10.1093/icesjms/fsv177.

Guan, X.Y., Liu, Y., Xie, D.X., 2018. Stability analysis of a Lotka-Volterra type predator-prey system with Allee effect on the predator species. Commun. Math. Biol. Neurosci. 2018, Article ID 9. 10.28919/cmbn/3654..

Hamre, J., 1991. Interrelation between environmental changes and fluctuating fish populations in the Barents Sea. In: Kawasaki, T., Tanaka, S., Toba, Y., Taniguchi, A. (Eds.), Long-term variability of pelagic fish populations and their environment. Pergamon Press, Oxford, UK, pp. 259–270.

Hanski, I., Henttonen, H., Korpimäki, E., Oksanen, L., Turchin, P., 2001. Small-rodent dynamics and predation. Ecology 82, 1505–1520. https://doi.org/10.1890/0012-9658.

Hanski, I., Turchin, P., Korpimäki, E., Henttonen, H., 1993. Population oscillations of boreal rodents: regulation by mustelid predators leads to chaos. Nature 364, 232–235. https://doi.org/10.1038/364232a0.

Holling, C.S., 1959. The Components of Predation as Revealed by a Study of Small-Mammal Predation of the European Pine Sawfly1. Can. Entomol. 91, 293–320. https://doi.org/10.4039/Ent91293-5.

Hunt Jr, G.L., McKinnell, S., 2006. Interplay between top-down, bottom-up, and wasp-waist control in marine ecosystems. Prog. Oceanogr. 68, 115–124. https://doi.org/10.1016/j.pocean.2006.02.008.

Ingvaldsen, R.B., Gjøsæter, H., 2013. Responses in spatial distribution of barents sea capelin to changes in stock size, ocean temperature and ice cover. Mar. Biol. Res. 9, 867–877. https://doi.org/10.1080/17451000.2013.775450.

Kroeker, K.J., Micheli, F., Gambi, M.C., 2013. Ocean acidification causes ecosystem shifts via altered competitive interactions. Nature Clim. Change 3, 156–159. https://doi.org/10.1038/nclimate1680.

Lotka, A.J., 1926. Elements of physical biology. Science Progress in the Twentieth Century (1919–1933) 21, 341–343. www.jstor.org/stable/43430362 (Accessed April 10, 2020)..

Muehlbauer, L.K., Schulze, M., Harpole, W.S., Clark, A.T., 2020. gauseR: Simple methods for fitting Lotka-Volterra models describing Gause's Struggle for Existence. bioRxiv 10.1101/2020.03.16.993642..

Nelder, J.A., Mead, R., 1965. A simplex method for function minimization. Comput. J. 7, 308–313. https://doi.org/10.1093/comjnl/7.4.308.

Rinaldi, S., Muratori, S., Kuznetsov, Y., 1993. Multiple attractors, catastrophes and chaos in seasonally perturbed predator-prey communities. Bltn Mathcal. Biol. 55, 15–35. https://doi.org/10.1016/S0092-8240(05)80060-6.

Ruan, S., 2009. On nonlinear dynamics of predator-prey models with discrete delay. Math. Model Nat. Phenom. 4, 140–188. https://doi.org/10.1051/mmnp/20094207.

Sarwardi, S., Haque, M., Mandal, P.K., 2012. Ratio-dependent predator-prey model of interacting population with delay effect. Nonlinear Dyn. 69, 817–836. https://doi.org/10.1007/s11071-011-0307-9.
Shampine, L.F., Thompson, S., 2001. Solving ddes in matlab. Appl. Numer. Math. 37, 441–458. https://doi.org/10.1016/S0168-9274(00)00055-6.
Solvang, H., Subbey, S., Frank, A.S.J., 2017. Causal Drivers of Barents Sea Capelin (Mallotus villosus) Population Dynamics on Different Time Scales. ICES J. Mar. Sci. 75, 621–630. https://doi.org/10.1093/icesjms/fsx179.
Stickney, A., 1991. Seasonal patterns of prey availability and the foraging behavior of arctic foxes (Alopex lagopus) in a waterfowl nesting area. Can. J. Zool. 69, 2853–2859. https://doi.org/10.1139/z91-402.
Tjelmeland, S., 1992. A stochastic model for the barents sea capelin stock with predation from an exogenous cod stock, in: Bogstad, B., Tjelmeland, S. (Eds.), Interrelations between fish populations in the Barents Sea. Institute of Marine Research, Bergen, Norway. Proceedings of the fifth PINRO-IMR Symposium, Murmansk, 12–16 August 1991, pp. 139–160..
Turchin, P., Hanski, I., 1997. An empirically based model for latitudinal gradient in vole population dynamics. Am. Nat. 149, 842–874.
Verhulst, P.F., 1838. Notice sur la loi que la population suit dans son accroissement. correspondance mathématique et physique publiée par a. Corresp. Math. Phys. 10, 113–121.
Volterra, V., 1926. Fluctuations in the abundance of a species considered mathematically. Nature 118, 558–560. https://doi.org/10.1038/118558a0.
WGIBAR, ICES, 2019. Report of the Working Group on Integrated Assessments of the Barents Sea (WGIBAR), February 2019, Murmansk, Russia. ICES CM0.

A. Frank is a postdoctoral research fellow at the University of Bergen, Norway, with interest in application of mathematical models to biological systems, perinatal pharmacoepidemiology, and causal inference methodology. Her current research deals with mathematical frameworks for empirical predator-prey systems, and macrophage polarization. She holds B.Sc. and M.Sc. degrees in mathematics from the Technical University of Munich, Germany, and a PhD from the University of Oslo, Norway.

S. Subbey is a principal research fellow at the Institute of Marine Research in Bergen, Norway, and adjunct professor at the Western Norway University of Applied Sciences, Norway. His research interests cover inverse and ill-posed problems in porous media physics, and bio-mathematics. Subbey's current research focuses on mathematical analysis of ecological systems when underlying drivers are vaguely understood, and system observations have modest accuracy.

M. Kobras is a Ph.D. student at the Centre for the Mathematics of Planet Earth, at the University of Reading. Her current research interest extends to the dynamics and variability of storm tracks in the midlatitude atmosphere and their response to slow climatic forcing, one of the key unknowns in future climate predictions. She holds a B.Sc. degree in Mathematics from FAU Erlangen. Her M.Sc. degree (Mathematics in Bioscience) is from the Technical University of Munich.

H. Gjøsæter is a principal research fellow at the Institute of Marine Research in Bergen, Norway. His main research interests are the ecology of the Barents Sea and adjacent Arctic marine areas. He has for many years been involved in stock assessment and management advice regarding various fish stocks in the Barents Sea and elsewhere. He holds a Dr. philos. from the University of Bergen, Norway dealing with various aspects of the biology of the Barents Sea capelin stock.